

HYPOEUTECTIC SILUMIN TO PRESSURE DIE CASTING WITH VANADIUM AND TUNGSTEN

The basic aim of this study is to investigate the effect of vanadium and tungsten on the crystallization process, microstructure and mechanical properties of silumin grade EN-AC 46000. The research involved a derivative thermal analysis DTA of the crystallization process, the metallographic analysis as well as the mechanical properties. The metallographic analysis was carried out on pressure die castings and made in the DTA probe. Vanadium and tungsten were added simultaneously to silumin in amount of approximately 0.1; 0.2; 0.3 and 0.4%. The DTA studies have shown the similar shape of all crystallization curves. It has been shown the additives of vanadium and tungsten in pressure die cast silumin can significantly increase its tensile strength as well as elongation.

Keywords: Multicomponent silumins, pressure die casting, DTA method

1. Introduction

Production of aluminum alloy castings remained at a high level in recent years. In 2012 fourteen million tonnes of Al alloy castings were produced. This comprised 13.9% of worldwide castings production. In 2013 and 2014, over 15 million tons and more than 16 million tons of aluminum alloy castings were produced, respectively. It comprised 14.9% and 15.5% of worldwide castings production [1-3]. Besides iron alloys, aluminum alloys are most commonly alloys group used for the casting production. The major interest in these alloys is mainly due to advantageous mechanical and technological properties either at low density. They are also characterized by relatively low production costs, mainly due to the relatively low melting temperature. Silumins are the typical representative aluminum alloys used in foundry engineering. Silumins wide application in industry requires continuous improvement of their mechanical and technological properties. These alloys are rarely casted into sand or ceramic moulds mainly due to their tendency to the formation of disadvantageous coarse grain microstructure because of relatively low heat transfer from the casting to mould. Much more often silumins are poured into permanent moulds or pressure casting dies. The more intensive heat transfer from the casting to metal mould leading to more favorable fine-grained microstructure. An intensification of the heat transfer from the casting can be also achieved using a suitable cooling medium to the metal mould [4]. Apart from the intensifying of the cooling rate the microstructure and properties of silumins can also be improved through their refining, modification, heat treatment, adding of alloying elements or the crystallization in a magnetic field [5-9]. Among the alloying elements, the elements with a high melting point such as chromium, molybdenum, vanadium

and tungsten can be distinguished. Research on aluminum alloys with these additives are described in papers [10-19]. According to the data contained in these papers, aforementioned elements are characterized by the lack of solubility in aluminum in the solid state. This results in the precipitation of intermetallic phases in the microstructure of silumins. These phases significantly increase the fragility of silumin. Very intensive heat transfer from casting reduces the probability of intermetallic phases forming, and reducing its quantity and size. This allows a supersaturation of the solid solution with alloying elements. The fastest heat transfer from the cast allows the pressure die casting. This is possible because of the thin-walled casting and the use of steel moulds with a volume substantially exceeding the casting volume. The supersaturation of solid solutions and, in particular, the phase α (Al) in silumin may cause its strengthening. For purposes of this study vanadium and tungsten were used as alloying additions. Accordingly, the aim of this study was to investigate the effect of vanadium and tungsten on the crystallization process, the microstructure and mechanical properties of hypoeutectic silumin to pressure die casting.

In Figure 1 Al-V equilibrium phase diagram is presented. There are six peritectic transformations leading to the formation of different intermetallic phases. The types of these phases and their crystallographic parameters are shown in Table 1.

From the data presented in Fig. 1 and Table 1 follows the solubility of vanadium in aluminum is negligible and amounts to maximum of 0.6 wt% (~0.3 at%). The maximum solubility of aluminum in vanadium is 54 at% at a temperature of about 1670°C. From Fig. 1 results even a slight addition of vanadium increases the crystallization temperature of Al-V alloy.

In Figure 2 Al-W equilibrium phase diagram is shown. Phases α , γ , δ and ϵ forms as a result of peritectic transformations occurring at the temperature of 697, 871 and

* LODZ UNIVERSITY OF TECHNOLOGY, DEPARTMENT OF MATERIALS ENGINEERING AND PRODUCTION SYSTEMS, 1/15STEFANOWSKIEGO STR., 90-924 ŁÓDŹ, POLAND

[#] Correspondence address: tomasz.szyczak@p.lodz.pl

1327°C, respectively. Crystallographic data of the phases in the Al-W equilibrium phase diagram are given in Table 2. The solubility of W in Al according to [20] is 0 wt%, and Al in W amounts to 2.2% at 1302°C. From W-V equilibrium phase diagram results both of elements form the solution with unlimited solubility in the solid state [20].

TABLE 1

Al-V Crystallographic data [20]

Phase	Composition, wt% V	Pearson Symbol	Space group
(Al)	0 do 0.3	<i>cF4</i>	<i>Fm$\bar{3}m$</i>
Al ₂₁ V ₂	~8.7 – 9.1	<i>mC104</i>	<i>C2/m</i>
Al ₄₅ V ₇	~13.5	<i>mP48</i>	<i>P2</i>
Al ₂₃ V ₄	~14.8	<i>mP180</i>	<i>P2/m</i>
Al ₃ V	~25	<i>aP30</i>	<i>P$\bar{1}$</i>
Al ₈ V ₅	39.5	<i>cI52</i>	<i>I$\bar{4}3m$</i>
(V)	~46 – 100	<i>cI2</i>	...
AlV ₃	~75	<i>cP8</i>	<i>R$\bar{3}m$</i>
β AlV ₃	~75	<i>h**</i>	...
α AlV ₃	~75	<i>t**</i>	...

TABLE 2

Al-W crystallographic data [20]

Phase	Composition, wt% V	Pearson Symbol	Space group
(Al)	0	<i>cF4</i>	<i>Fm$\bar{3}m$</i>
γ	~37	<i>Ci26</i>	<i>Im$\bar{3}$</i>
d	~58 – 60	<i>hP12</i>	<i>P6₃</i>
ϵ	~62 – 66	<i>mC30</i>	<i>Cm</i>
W	100	<i>cI2</i>	<i>Im$\bar{3}m$</i>

2. Experimental (Materials and Methods)

To the study the hypoeutectic silumin to pressure die casting EN-AC 46000 (EN-AC AlSi9Cu3(Fe)) was used [21]. Its chemical composition is given in Table 3. Silumin was melted in a gas shaft furnace with a capacity of 1.5 tons. Silumin was refining within the shaft furnace with use of solid refiner Ecosal Al 113.S. Approx. 0.25 kg of refiner per 500 kg of the melt was used. After tapping, the silumin was poured from the furnace into a ladle with a capacity 300 kg and deslagged with using Ecremal N44 slag trap. As a next, one measuring spoon of ZUDX-5501 slag trap per 300 kg of silumin inside the ladle was added. After smelting and refining silumin was transported to the holding furnace set near to Idra 700S pressure machine with a horizontal cold chamber. Into silumin AlV10 and AlW8 master alloys were added in the holding furnace. Silumin temperature in the holding furnace amounted to 750°C. The liquid alloy with master alloys was held by 20 minutes. Amount of silumin and master alloys were chosen in such a way to give a concentration of approximately 0.1; 0.2; 0.3 and 0.4% V and W each of them. As part of this study silumin grade EN-AC 46000 without the addition of vanadium and tungsten was also studied. For each variant of chemical composition the housing roller blinds castings were made with predominant wall thickness of 2 mm. The research was performed under the production conditions of the Innovation and Implementation Enterprise Wifama-Prexer Ltd., Poland. Derivative thermal analysis (DTA) method was used to examination of the crystallization process. The DTA method have been used to study iron, aluminum, bronze, magnesium and cobalt alloys [22-25]. For recording DTA curves PtRh10-Pt thermocouple placed inside the DTA10-TUL probe was used. The probe was made of the resin sand. Its dimensions are shown in Figure 3. Before the pouring the tested silumin was overheating to temperature of 1100°C. The high overheating of the alloy is dictated by the large heat losses during silumin transfer from furnace to TDA probe and the possibility of increase the liquidus temperature by V and W additives.

TABLE 3

The chemical composition of EN-AC 46000 silumin

Chemical composition, wt%										
Si	Fe	Cu	Mn	Mg	Cr	Ni	Zn	Pb	Sn	Ti
8.66	0.86	2.36	0.23	0.33	0.04	0.11	0.93	0.09	0.03	0.05

For each tested chemical composition three specimens were cut out from one casting. They had a rectangular cross section with dimensions of 2/10 mm as is recommended by the standard [21]. Tensile tests were performed on Instron 3382 machine using a speed 1 mm/min. During the tensile

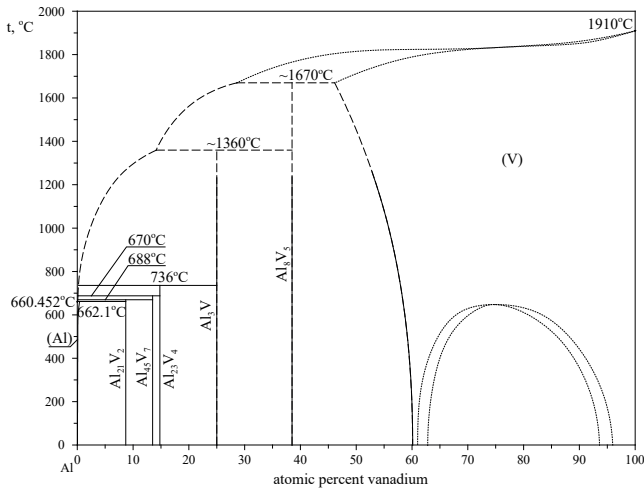


Fig. 1. Aluminum-vanadium phase diagram [20]

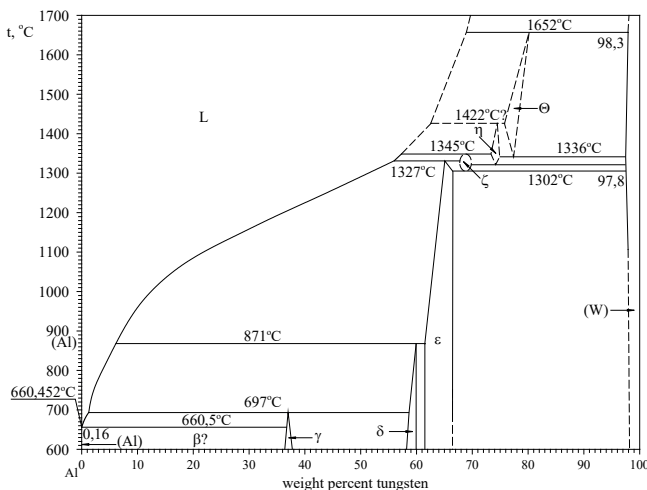


Fig. 2. Aluminum-tungsten phase diagram [20]

tests tensile strength R_m , yield strength $R_{p0.2}$ and elongation A were determined. Hardness tests were performed on Briviskop HPO-2400. The ball with a diameter of $d = 2.5$ mm and a load of 613 N was used to the test.

Silumin microstructure was investigated on samples taken from pressure castings as well as from DTA probe. Metallographic specimens were etched with 2% aqueous solution of HF and tested at a magnification of $\times 100$ and $\times 1000$ on metallurgical microscope Nikon Eclipse MA200.

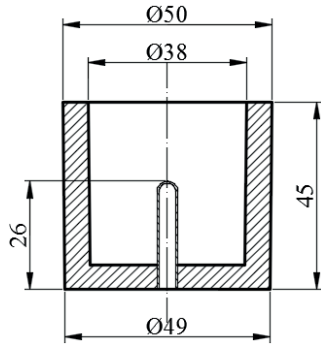


Fig. 3. DTA10-TUL probe dimensions

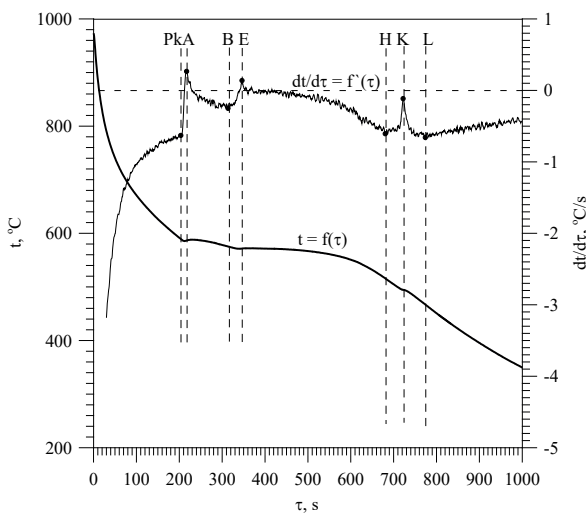


Fig. 4. DTA curves of EN-AC 46000 silumin without V and W

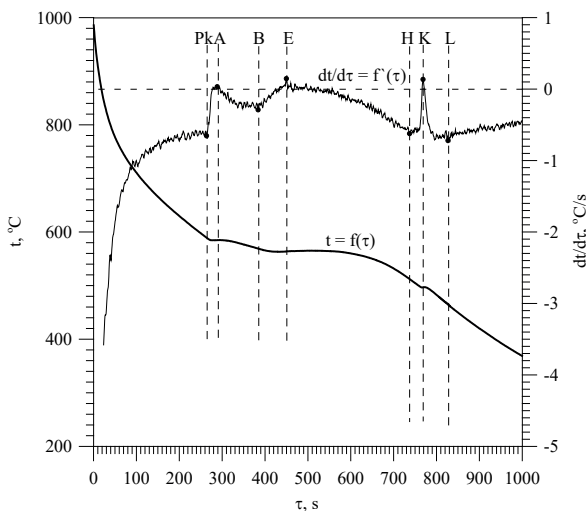


Fig. 5. DTA curves of EN-AC 46000 with 0.4% of vanadium and tungsten (each of them)

3. Results and discussion

Figure 4 shows the DTA curves of silumin EN-AC 46000 without the addition of vanadium and tungsten. There are three thermal effects on it. The first thermal effect designated as PkAB comes from the crystallization of the solid solution $\alpha(\text{Al})$ dendrites. The next thermal effect described as BEH comes from the triple eutectic $\alpha + \text{Al}_9\text{Fe}_3\text{Si}_2 + \beta$, while HKL thermal effect corresponds to the quadruple eutectic $\alpha + \text{Al}_2\text{Cu} + \text{AlSiCuFeMgMnNiTi} + \beta$. Studies of the crystallization process as well as the microstructure of silumin 226 grade are described in [18]. 226 silumin is an equivalent to EN-AC 46000 silumin included in DIN 1725-2/1986. The interpretation of the characteristic points on the DTA curves is as follows: Pk – crystallization start; A, E and K – maximum thermal effects from crystallization of: solid solution α , triple and quadruple eutectic, respectively, B – α phase crystallization finish and start of the triple eutectic crystallization, simultaneously, H – crystallization finish of the triple eutectic and start of the quadruple eutectic mixture crystallization, L – crystallization finish of the quadruple eutectic. The temperature values “t”, and the cooling rate “dt/dτ” in the characteristic points of the tested silumin are given in Table 4. Data presented in the Tab. 4 indicated α solid solution crystallizes in the temperature range $t_{Cs} = 588^\circ\text{C}$ to $t_B = 575^\circ\text{C}$. At the temperature t_B triple eutectic mixture crystallization start takes place. At $t_H = 516^\circ\text{C}$ its crystallization finish can be found as well as the crystallization start of the quadruple eutectic. The finish of the quadruple eutectic crystallization process occurs at a temperature $t_L = 467^\circ\text{C}$. Vanadium and tungsten additives in the tested silumin does not change the DTA curves run. For each tested chemical composition there are similar thermal effects. The differences consist in coordinate values of the characteristic points on the curves. It is shown in Table 4. From data in Tab. 4 results there is no an unequivocal effect of vanadium and tungsten on values of the temperature “t” and the cooling rate “dt/dτ” at the characteristic points.

TABLE 4

Values of the temperature (a) and cooling rate (b) at the characteristic points

V and W concentration, wt%	Temperature t , °C						
	Cs	A	B	E	H	K	L
0.0	588	586	575	572	516	495	467
0.1	587	583	574	572	514	495	466
0.2	595	582	577	570	516	492	465
0.3	595	585	574	573	515	494	467
0.4	593	585	571	564	512	497	465

V and W concentration, wt%	dt/dτ, °C/s						
	Cs	A	B	E	H	K	L
0.0	-0.63	0.26	-0.25	0.14	-0.61	-0.11	-0.66
0.1	-0.61	0.23	-0.24	0.05	-0.60	-0.13	-0.67
0.2	-0.70	0.14	-0.23	0.04	-0.63	-0.18	-0.70
0.3	-0.64	0.14	-0.22	0.10	-0.61	-0.18	-0.60
0.4	-0.65	0.03	-0.27	0.15	-0.62	0.09	-0.72

The DTA curves of silumin with the addition of vanadium and tungsten is shown in Figure 5. Due to the lack of vanadium and tungsten solubility in aluminum at the ambient air temperature, and a relatively slow crystallization process in the DTA probe as well as no occurrence of the additional thermal effects on the DTA curves it should be assumed that vanadium and tungsten are located inside intermetallic phases. The most likely is their occurrence in the most complex quadruple eutectic. Therefore, in silumins containing V and W it should take a form $AlSiCuFeMgMnNiTiVW$.

Figure 6 presents the microstructure of EN-AC 46000 silumin poured into the DTA probe. It complies with the previously presented crystallization process described with use of the DTA curves. Therefore there are α dendrites of the solid solution, triple eutectic $\alpha + Al_9Fe_3Si_2 + \beta$ as well as the quadruple eutectic mixture $\alpha + Al_2Cu + AlSiCuFeMgMnNiTi + \beta$. The microstructure of the silumin containing V and W obtained in the DTA probe is presented in Figure 7 (a-d). The presented data show there are new phases in silumin containing approximately 0.2; 0.3 and 0.4% V and W. They do not appear in the silumin without vanadium and tungsten, and containing 0.1% of these additives. They are probably intermetallic phases containing V and W which crystallize during peritectic transformations. The identification of phases in Al-Si alloys containing Cr, V, W, and Mo is presented inter

alia in [7, 13, 15, 26]. Their size is relatively small compared with other elements of the microstructure and usually did not exceed 50 μm . The relatively small amount of aforementioned precipitates did not cause additional thermal effect on the DTA curves (Fig. 5).

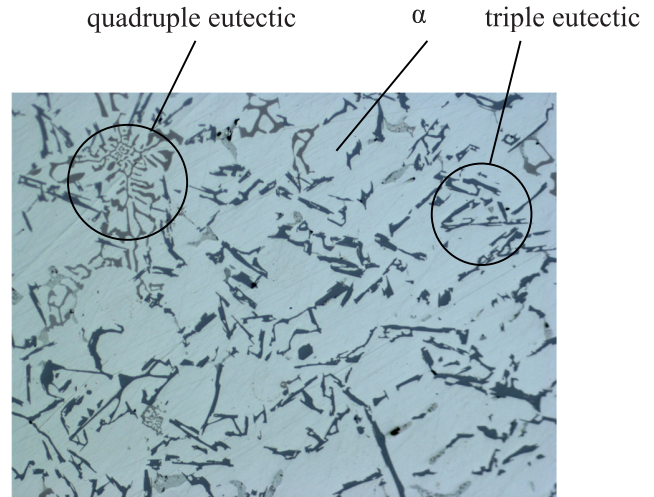


Fig. 6. Microstructure of EN-AC 46.000 silumin obtained in the DTA probe: $\alpha, \alpha + Al_9Fe_3Si_2 + \beta, \alpha + Al_2Cu + AlSiCuFeMgMnNiTi + \beta$

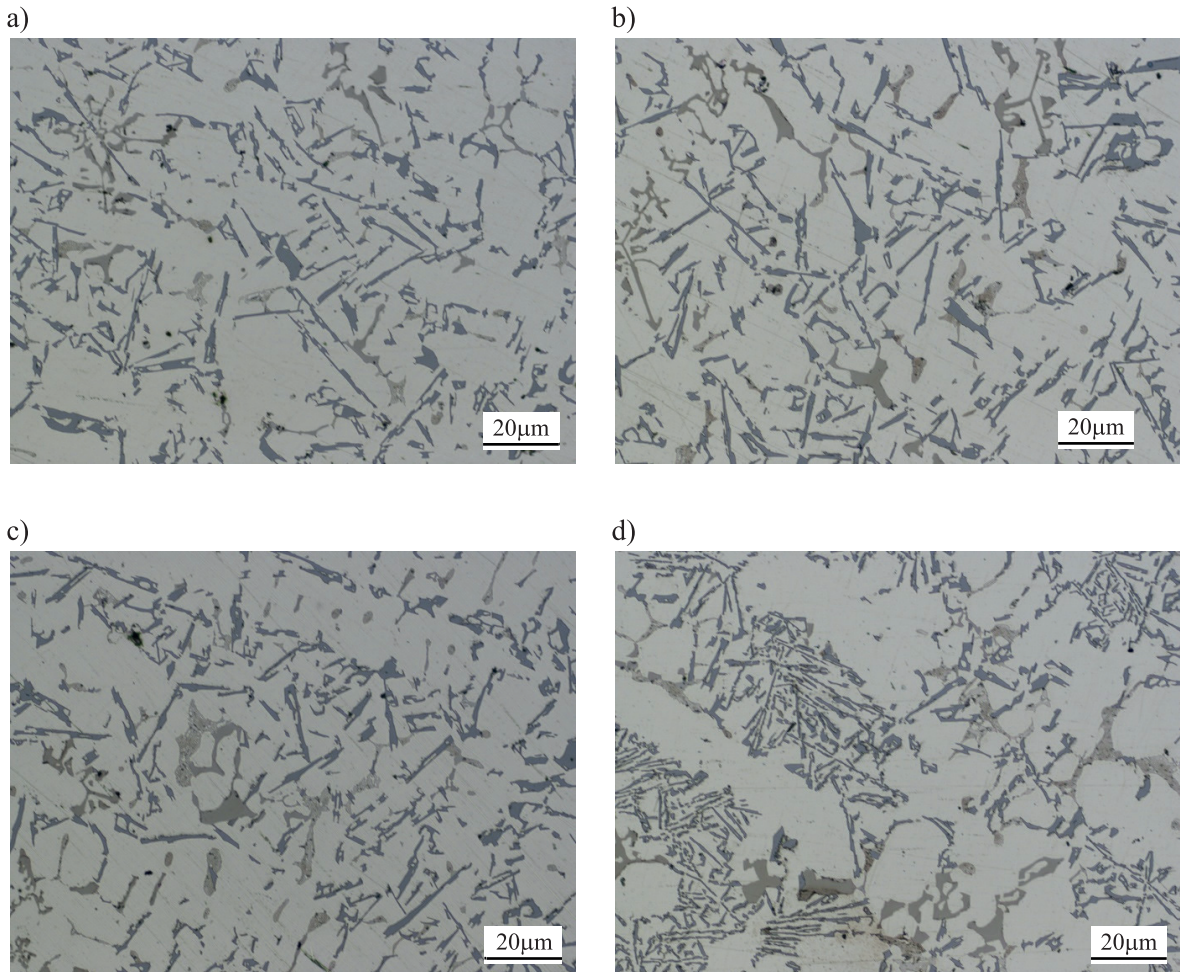


Fig. 7 (a-d). The microstructure of the silumin with tungsten and vanadium obtained in DTA probe: a – 0.1%; b – 0.2%; c – 0.3%; d – 0.4%: $\alpha, \alpha + Al_9Fe_3Si_2 + \beta, \alpha + Al_2Cu + AlSiCuFeMgMnNiTiVW + \beta$

Figure 8 presents the microstructure of EN-AC 46000 silumin without vanadium and tungsten obtained in the pressure die casting. As regards the type of the phases it is similar to microstructure obtained in the DTA probe. The difference comes down to the size and number of $\text{Al}_9\text{Fe}_3\text{Si}_2$ and Al_2Cu intermetallic phases precipitates. The microstructure of the pressure die casting is characterized by greater size reduction of the phases precipitation and its greater amount in relation to the casting from the DTA probe. It is connected with the very intense thermal conductivity from cast to the pressure casting die. It resulting in not only size reduction of the microstructure components but also non-equilibrium character of the crystallization process. Consequently, there is a supersaturated solid solution with alloy additions, in particular, copper and iron.

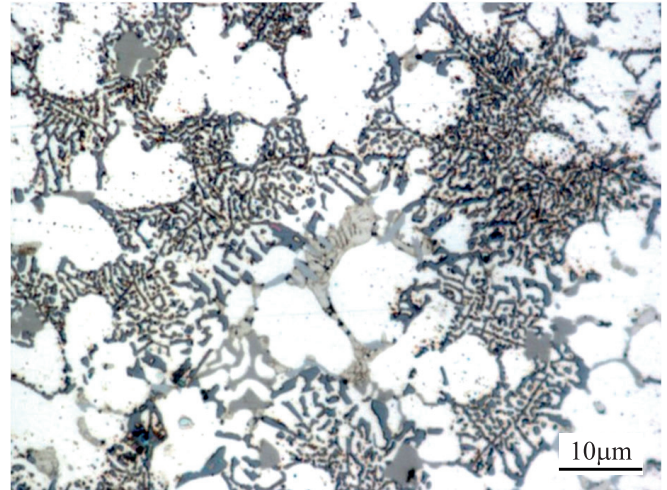


Fig. 8. Microstructure of EN-AC 46.000 silumin in the pressure die casting: α , $\alpha + \text{Al}_9\text{Fe}_3\text{Si}_2 + \beta$, $\alpha + \text{Al}_2\text{Cu} + \text{AlSiCuFeMgMnNi} + \beta$

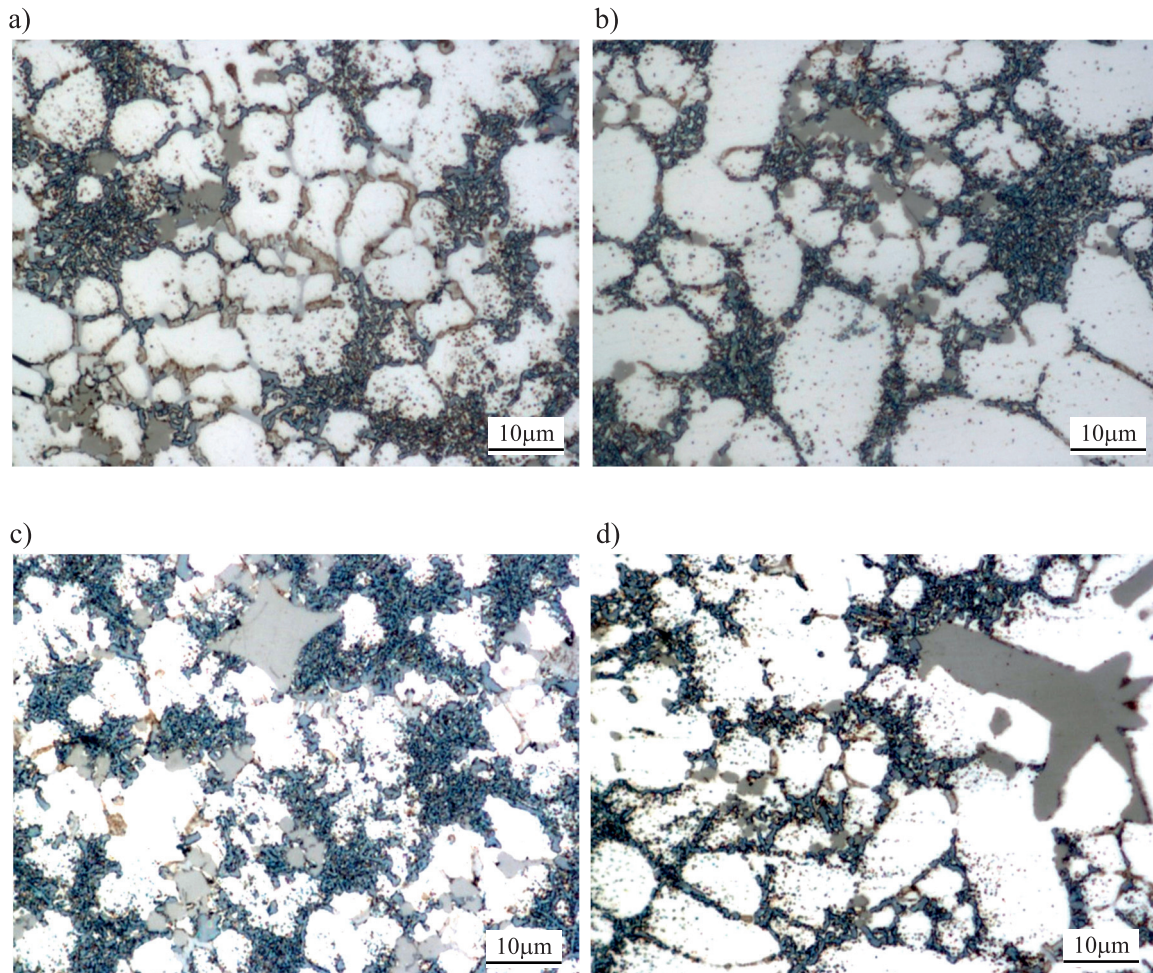


Fig. 9 (a+d). The microstructure of pressure die castings made of the tested silumin with the addition of V and W in an amount of approximately: a - 0.1%; b - 0.2%; c - 0.3%; d - 0.4%: α , $\alpha + \text{Al}_9\text{Fe}_3\text{Si}_2 + \beta$, $\alpha + \text{Al}_2\text{Cu} + \text{AlSiCuFeMgMnNiTiVW} + \beta$

The microstructure of pressure die casting made of silumin containing vanadium and tungsten is shown in Figure 9 (a-d). The additives of vanadium and tungsten resulted in the occurrence of additional phases, similarly as it was in silumins with 0.2; 0.3 and 0.4% V and W poured into the DTA probe. Aforementioned phases in alloy containing 0.1 and 0.2% V and W are characterized by relatively small size, generally not exceeding 5 μm . At a concentration of 0.3% V and W they reached $\sim 20 \mu\text{m}$, while for a concentration of 0.4% even more than 30 μm . These phases together with dendrites of α solid solution are the biggest elements of the microstructure of the silumin containing approximately 0.3 and 0.4% V and W. They significantly exceed the size of other phases, in particular β solid solution coming from the eutectic mixtures. These crystals have a morphology similar to the walled, with sharp edges.

The mechanical properties of the tested silumins without and with vanadium and tungsten are presented in Table 5 and in Figure 10 (a-c). From the presented data results a significant effect of above-mentioned elements on the tensile strength R_m as well as elongation A. These additives do not significantly affect on the yield strength $R_{p0.2}$ and hardness HB. The lowest values of $R_m = 197 \text{ MPa}$ and $A = 1.8\%$ was obtained for unalloyed silumin. An addition of V and W across the range tested initially resulted in an increase in R_m and A value and as a next its reduction. The highest values of $R_m = 299 \text{ MPa}$ was achieved for 0.2% and 0.3 V and W, and the maximum elongation $A = 6.3\%$ for 0.2% V and W. Relatively fast crystallization process of silumin inside the pressure casting

die presumably causes the supersaturation of the solid solutions with vanadium and tungsten (in particular the α phase). It should be assumed R_m and A values increase with increasing the phase α supersaturation. The excess of vanadium and tungsten causes intermetallic phases precipitation containing these elements. The presence of the relatively large precipitates in the microstructure leads to a reduction in the R_m and A values

TABLE 5
Mechanical properties of EN-AC 46000 without and with V and W

V and W concentration, wt%	Mechanical properties			
	R_m , MPa	$R_{p0.2}$, MPa	A, %	HB
0.0	197	122	1.8	112
0.1	275	119	4.4	114
0.2	299	119	6.3	114
0.3	299	117	5.7	113
0.4	245	132	3.4	111

4. Conclusion

From the data included in this paper the following conclusions can be drawn:

- independently from the concentration of tungsten and

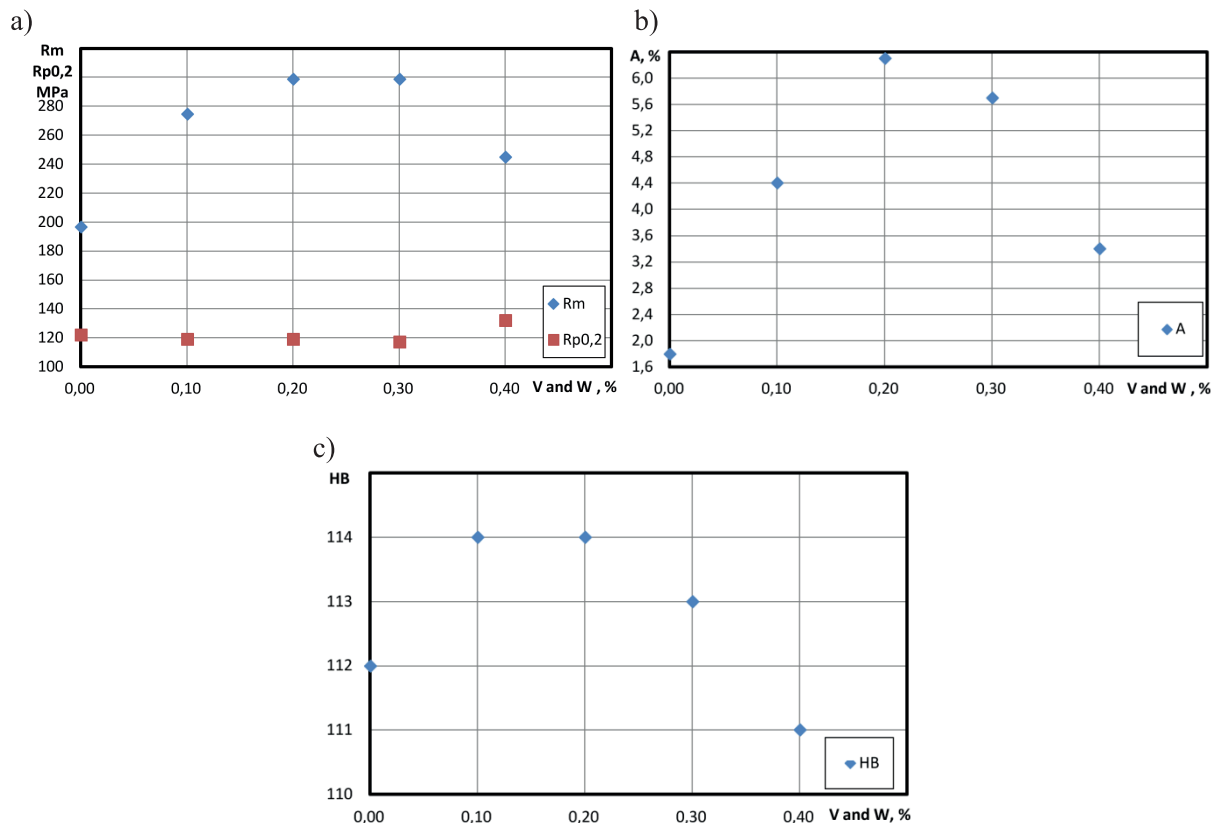


Fig. 10 (a-c). Mechanical properties of EN-AC 46000 without and with V and W

vanadium there are three similar thermal effects on DTA curves coming from the crystallization of: solid solution α , triple and quadruple eutectic,

- vanadium and tungsten cause the occurrence of the intermetallic phases with morphology similar to walled in the microstructure of silumin from DTA probe as well as pressure die casting,
- the highest values of tensile strength $R_m = 299$ MPa was obtained for 0.2 and 0.3% V and W, and an elongation $A = 6.3\%$ for 0.2% of the aforementioned additives,
- an increasing in the tensile strength as well as an elongation of pressure die casting silumin is likely the result of supersaturation of α solid solution additions of vanadium and tungsten,
- the decrease in the R_m and A values is probably caused by relatively large intermetallic phases precipitations containing vanadium and tungsten.

Acknowledgement

Project co-financed by the European Regional Development Fund under the Operational Programme Innovative Economy in 2013-2015 according to the agreement No. UDA-POIG.01.04.00-10-079/12.

REFERENCES

- [1] 47th Census of World Casting Production. Mod. Cast. 18-23 (December 2013).
- [2] 48th Census of World Casting Production. Mod. Cast. 17-21 (December 2014).
- [3] 49th Census of World Casting Production. Mod. Cast. 26-31 (December 2015).
- [4] R. Władysiak, Arch. Metall. Mater. **58** (3), 977-980 (2013).
- [5] J. Pezda, Metalurgija **53** (1), 63-66 (2014).
- [6] J. Piątkowski, B. Formanek, Mater. Sci. Eng. **22**, 012020 (2011).
- [7] S. Pietrowski, Silumins, 2001 Publishing house of Lodz University of Technology, Łódź.
- [8] J. Piątkowski, Sol. St. Phen. **203-204**, 417-422 (2013).
- [9] T. Wróbel, J. Szajnar, Arch. Metall. Mater. **58** (3), 941-944 (2013).
- [10] F. Binczyk, J. Piątkowski, Archives of Foundry **3** (9), 39-44 (2003).
- [11] K.L. Sahoo, B.N Pathak, J. Mater. Process. Tech. **209**, 798-804 (2009).
- [12] K.L. Sahoo, S.K. Das, B.S. Murty, Mater. Sci. Eng. **355** (1-2), 193-200 (2003).
- [13] S. Pietrowski, R. Władysiak, B. Pisarek, in: S. Pietrowski (Ed.), Proceedings of the International Conference Light Alloys and Composites. (pp. 77-83), 13-16 May 1999.
- [14] S. Pietrowski, R. Władysiak, B. Pisarek, Solidification of Metals and Alloys **13**, 103-108 (1998).
- [15] S. Pietrowski, T. Szymczak, Arch. Foundry Eng. **9** (3), 143-158 (2009).
- [16] S. Pietrowski, T. Szymczak, B. Siemińska-Jankowska, A. Jankowski, Arch. Foundry Eng. **10** (2), 107-126 (2010).
- [17] S. Pietrowski, T. Szymczak, Modification of silumins with alloying elements, in S. Pietrowski (Eds.), Tendencies of optimization of the production system in foundries, Katowice-Gliwice: PAN 2010.
- [18] T. Szymczak, G. Gumienny, T. Pacyniak, Transactions of the Foundry Research Institute **55** (3), 3-14 (2015).
- [19] T. Szymczak, G. Gumienny, T. Pacyniak, Arch. Foundry Eng. **15** (4), 81-86 (2015).
- [20] Alloy Phase Diagrams. ASM Handbook. 3 (1992).
- [21] PN EN 1706:2010 Aluminium And Aluminium Alloys - Castings - Chemical Composition And Mechanical Properties.
- [22] S. Pietrowski, B. Pisarek, R. Władysiak, G. Gumienny, T. Szymczak, TDA curves of metals alloys and the control of their quality, in Szajnar J. (Eds.), Advances In Theory and Practice Foundry, Katowice-Gliwice: PAN 2009.
- [23] B.P. Pisarek, Arch. Foundry Eng. **13** (3), 72-79 (2013).
- [24] C. Rapiejko, B. Pisarek, E. Czekaj, T. Pacyniak, Arch. Foundry Eng. **14** (1), 97-102 (2014).
- [25] B. Kacprzyk, T. Szymczak, G. Gumienny, L. Klimek, Arch. Foundry Eng. **13** (3), 47-50 (2013).
- [26] S. Pietrowski, Complex silumins. Journal of Achievements in Materials and Manufacturing Engineering **24** (1), 101-105 (2007).

